



Topology optimization of steel shear fuses to resist buckling

Javier A. Avecillas¹, Matthew R. Eatherton²

Abstract

Shear-acting structural fuses are steel plates subjected to in-plane lateral displacements during extreme loading events such as earthquakes, that dissipate energy through localized shear or flexural yielding mechanisms. Although previous studies have reported that fuses with specific geometry can develop a stable hysteretic behavior, their small thickness makes them prone to buckling which reduces strength and energy dissipation capacity.

In this work, topology optimization using a genetic algorithm is performed to find optimized shapes for structural fuses to yield while resisting buckling. The objective function uses the fuse's shear buckling load (V_B) obtained from an eigenvalue analysis, and shear yield load (V_Y) obtained from a material nonlinear, but geometrically linear 2D plane stress analysis. The two types of analysis are shown to be computationally efficient and viable for use in the optimization routine. A new set of optimized topologies are obtained, interpreted into smooth shapes, and analyzed to evaluate their effectiveness. The computational results show that the optimized topologies present a stable hysteretic behavior through cycles of large drift angles with well localized yielding mechanisms.

1. Introduction

A recent approach to the design of seismic force resisting systems consists of concentrating inelastic deformations in structural fuses that are thin steel plates with cutouts which dissipate energy through local yielding mechanisms. These structural fuses can be used as the ductile mechanism in a self-centering steel braced frame, as the shear link in an eccentrically braced frame, or in a damper configuration as illustrated in Fig. 1. However, these steel plates are affected by buckling-related phenomena such as out-of-plane deformations, pinched hysteretic behavior, low lateral force resistance during load reversals, and reduced energy dissipation capacity.

Several different strategies have been used to mitigate buckling in structural fuses. One approach is to use stiffeners that partially or totally cover the energy dissipation zone of a structural fuse, thus reducing the out-of-plane deformations (e.g. Deng et al. 2015). Another philosophy to prevent buckling is to use cutout patterns. For instance, a fairly ductile hysteretic behavior in

¹ Graduate Research Assistant, Virginia Tech, <javec@vt.edu>

² Associate Professor, Virginia Tech, <meather@vt.edu>

structural fuses is obtained by including diamond-shape openings that create butterfly-shape links (e.g. Ma et al. 2010). Along the same lines, a ring-shape structural fuse was conceived to prevent shear buckling by eliminating the slack in the plate perpendicular to the tension field direction (Egorova et al. 2014). Topology optimization has also been implemented to improve the cyclic performance of a structural fuse, but has not explicitly addressed buckling. By minimizing the worst cumulative plastic strain (Liu and Shimoda 2013) or maximizing the dissipated energy by the structural fuse (Ghabraie et al. 2010), new topologies with an enhanced hysteretic behavior haven been discovered.

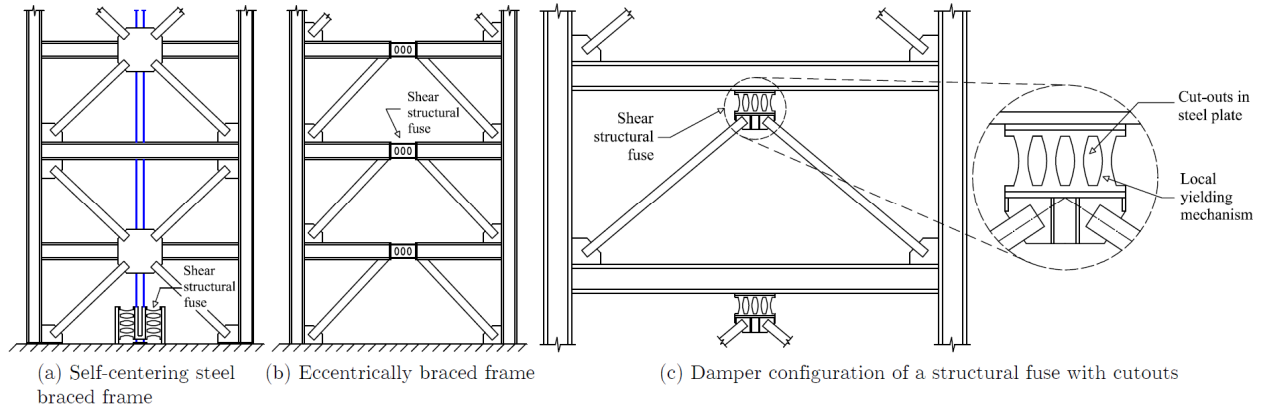


Figure 1: Seismic force resisting systems using steel shear fuses

In this study, an objective function is proposed in conjunction with a topology optimization algorithm to obtain new cutout patterns in a square domain of constant thickness that will help a structural fuse resist buckling. Results are presented from three runs of the optimization procedure with variations on the objective function that control the buckling resistance, and resulting topologies are obtained. The new topologies are interpreted into smooth shapes and evaluated using finite element analyses. Finally, their cyclic behavior, energy dissipation ability and damping capacity are compared against previously studied shear structural fuses.

2. Development of an objective function

The purpose of topology optimization is to find an optimum distribution of material within a design space given a set of loads, boundary conditions and performance targets. In this case, the design space consists of a square plate with constant thickness, as illustrated in Fig. 2(a). The boundary conditions correspond to a structural fuse with a fixed bottom edge and an applied horizontal displacement at the top edge. Also, one of the constraints described in this paper is setting the volume of the optimized topology to 40% of the full domain. See Avecillas (2018) for other volume fractions.

The performance target is described by the objective function given in Eq. 1. The numerator consists of a normalizing term where the yield stress is taken as, $F_Y=345$ MPa, the width of the domain is, $w=711$ mm, the plate thickness is, $t=12.7$ mm, and the volume fraction is, $\Delta=40\%$. Since the goal of the topology optimization is to resist buckling, the denominator includes a term that is an exponential function of $V_Y/V_B - k$. In this expression, V_B , is the shear buckling load obtained from an eigenvalue analysis, V_Y , is the shear yield load obtained by a planar 2D analysis with nonlinear material properties, and k is the target value of V_Y/V_B . The goal of the exponential term is to produce a topology with a shear yield load V_Y , less than the elastic shear buckling load

V_B , where small values of k such as $k = 0.1, 0.2, 0.3$, imply considerable yielding before buckling occurs. The second term in the denominator incentivizes larger values of V_Y and V_B . To summarize, a graphic illustration of the objective function is presented in Fig. 2(b) where darker areas represent the most optimal combinations of V_Y and V_B . The figure demonstrates the objective function for a value of $k=1$, but smaller values of k ($k=0.1$ through 0.3) are used in the optimization.

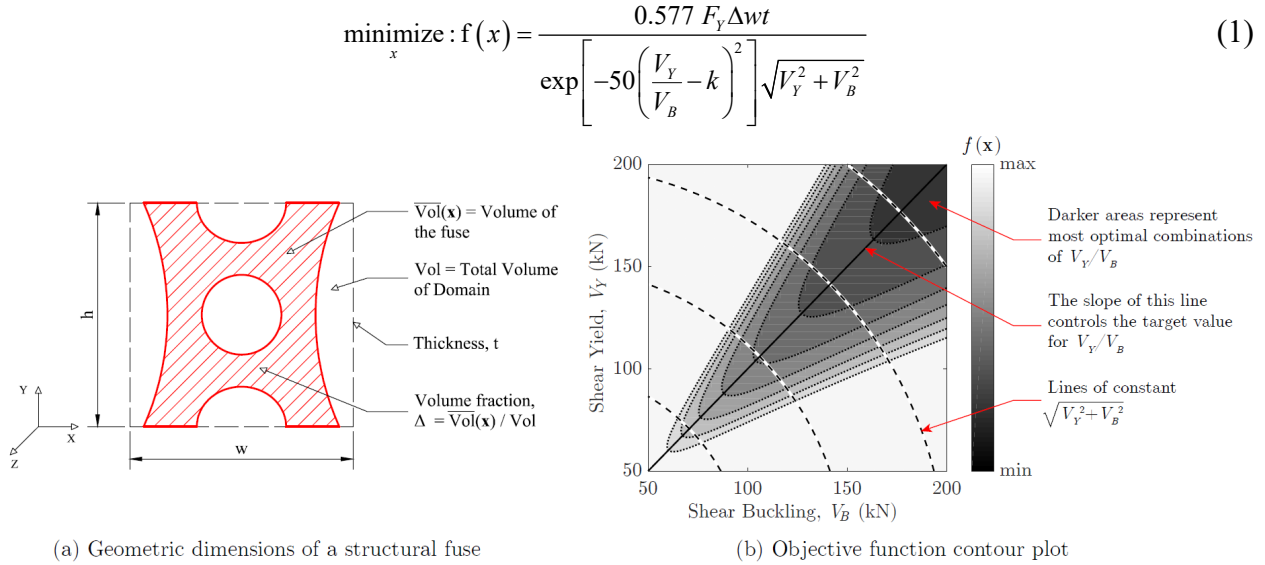


Figure 2: Geometric dimension of a structural fuse and graphic representation of the objective function

The topology is represented using a binary approach, where the presence of material is associated with the number one (1) and the existence of void with the number zero (0), as shown in Fig. 3. During the optimization procedure, input vectors that represent topologies with disconnected components are considered non-admissible. In order to fix those topologies, a repair algorithm is performed only if the largest component of the topology contains at least 90% of the target volume (Madeira et al. 2006). An image-processing-based analysis is performed to find topologies that lack a load path (Avecillas 2018), which are also considered non-admissible. Those shapes considered as non-admissible are not discarded from the optimization process but assigned an objective function value equal to 1.01 times the worst objective function value from the admissible shapes.

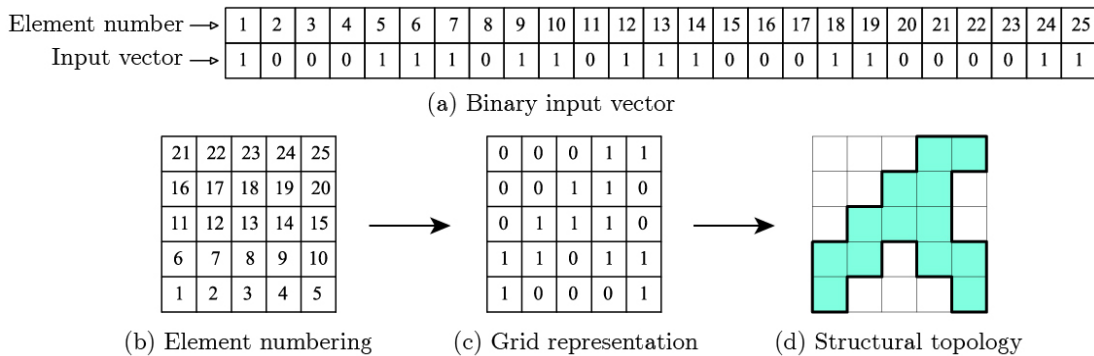


Figure 3: Binary representation of a topology

For those topologies that pass the admissibility filters such as the structural fuse illustrated in Fig. 4(a), two computationally inexpensive FE analyses are performed using the software called Finite Element Analysis Program or FEAP (Taylor 2013). The elastic shear buckling load V_B , is obtained from a three-dimensional elastic eigen-buckling analysis considering the FE model and boundary conditions illustrated in Fig. 4(b). Since structural fuses are doubly-symmetric in terms of shape and boundary conditions, only one quarter or the domain is used to calculate the shear yield load, V_Y , where a two-dimensional plane-stress FE analysis with non-linear material is performed, as show in Fig. 4(c). The material properties used in the FE analyses correspond to ASTM A572 Grade 50 steel plate with Young's modulus of $E=200,000$ MPa, Poissons ratio of $\nu=0.3$, yield strength of $F_Y=345$ MPa, linear kinematic hardening rule, and a hardening slope equal to $H=2,000$ MPa.

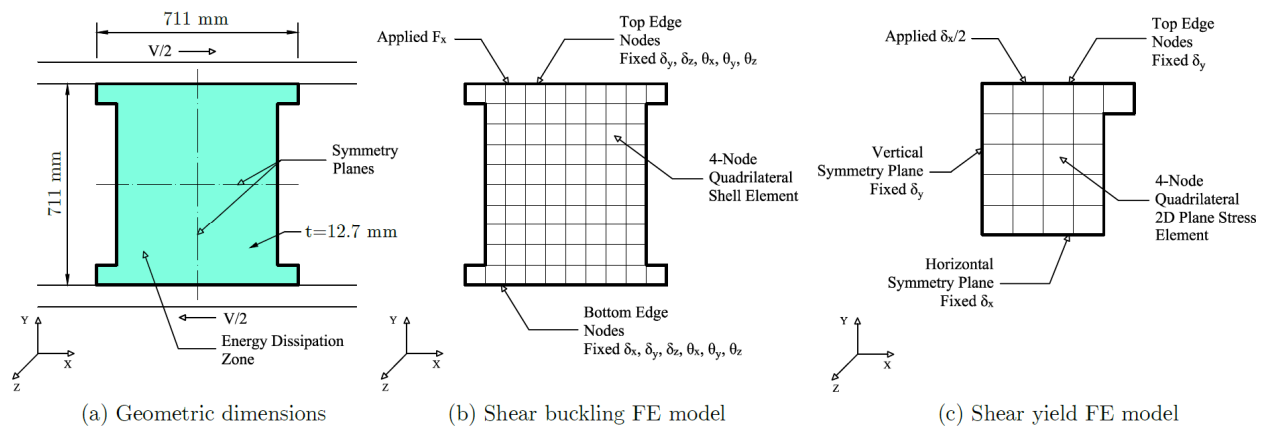


Figure 4: Seismic force resisting systems using steel shear fuses

3. Topology optimization of structural fuses

3.1 Optimization setup

The optimization procedure uses a genetic algorithm written in Matlab. The initial population consists of 100 topologies that meet the target 40% volume fraction including 95 randomly generated shapes, 1 topology representing the ring-shape structural fuse (Egorova et al. 2014), 3 variations of the butterfly fuse (Ma et al. 2010), and an X-shape topology representing the topology with the maximum in-plane stiffness (Sigmund 2001). See Avecillas (2018) for more details. All topologies use a square domain of 711 mm by 711 mm and thickness equal to 12.7 mm, discretized with a 32 by 32 square finite element mesh. An extra row of seed elements is added to the top and bottom edge of the domain to facilitate the application of boundary conditions, although these extra elements are not part of the optimization procedure.

The genetic algorithm is run for 400 generations and uses an exponential ranking selection with an exponent equal to 0.8, a single-point crossover operation that interchanges 50% of the topology's structure, a 5% probability of mutation interchanging 10% of the topology volume, and an elitism condition where the top 4% of topologies are retained for the next generation. For the parameters of the study described in this paper (e.g. objective function, domain, volume fraction), this combination of genetic operators produced the best results in terms of average final objective function value, convergence rate and number of admissible topologies (Avecillas 2018). Also, to produce a doubly-symmetric structural fuse, the genetic algorithm only operates

with one quarter of the actual topology. The algorithm does not have a special consideration for eliminating or consolidating repeated topologies.

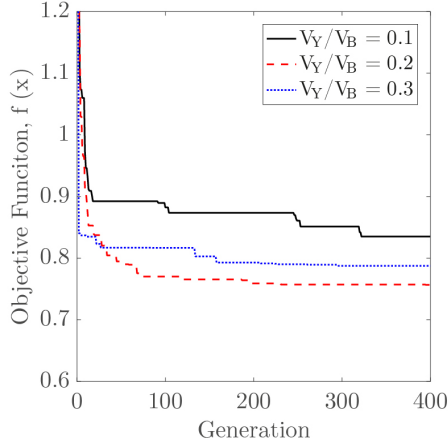
3.2 Topology optimization results

The evolution of the objective function value for the best topology in each generation during the optimization process is illustrated in Figure 5(a). It is observed that the optimization procedures with $k=0.2$ and 0.3 , have a relatively fast convergence rate until the algorithm reaches a value of the objective function near its final value after approximately generation 200. Although the evolutionary process for $k=0.1$ seems to rapidly improve the objective function value during initial generations, the value continues to improve even after generation 300 so it is not clear whether the algorithm fully converged. On the other hand, Fig. 5(b) shows that the value of k does not influence the number of admissible topologies during the optimization process, since in all the cases the number of admissible topologies rapidly increases to a relatively constant average of 70 useful shapes during each generation.

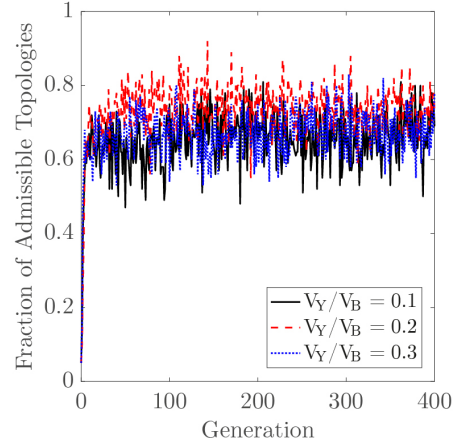
The values of the elastic shear buckling load V_B , shear yield load V_Y , and objective function $f(x)$, associated with the best candidate topology at the end of the evolutionary process are presented in Table 1. It is observed that regardless of the prescribed value of k , the genetic algorithm produces a final topology with about the same elastic buckling load but different shear strength. This similarity in terms of buckling capacity can be explained by the shape of the optimized structural fuses illustrated in Fig. 5(c) to Fig. 5(e). Although the yielding mechanism may vary, two solid legs linked together by weaker elements appear to be the optimized geometrical configuration for resisting buckling. Furthermore, the buckling load does not seem to be able to increase much past 900 kN for any topology with a 40% volume fraction.

Table 1: Numerical results of the optimization procedure

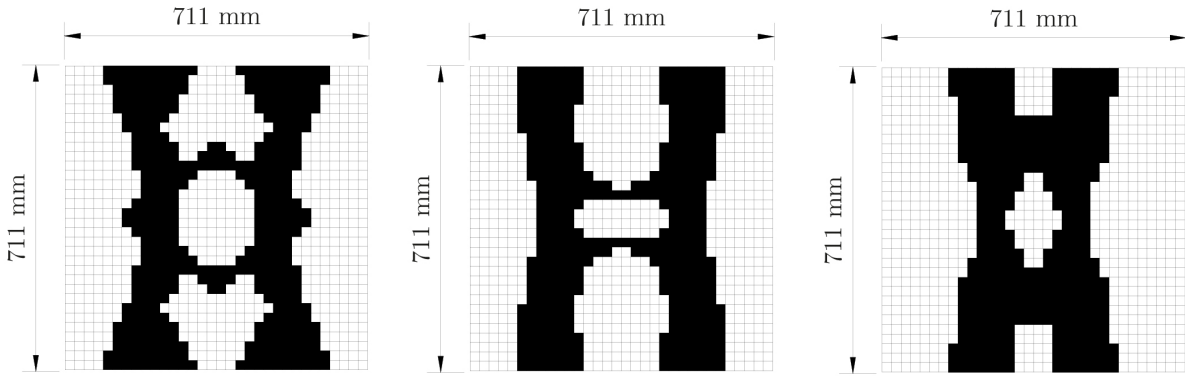
k (Target V_Y/V_B)	V_B (kN)	V_Y (kN)	$f(x)$
0.1	865.6	99.9	0.835
0.2	932.8	184.3	0.757
0.3	887.9	267.3	0.787



(a) Evolution of the Objective Function



(b) Evolution of the Fraction of Admissible Topologies



(c) Optimized Topology - $V_Y/V_B=0.1$ (d) Optimized Topology - $V_Y/V_B=0.2$ (e) Optimized Topology - $V_Y/V_B=0.3$

Figure 5: Results of the optimization procedure for a target volume of 40% of the full domain

4. Cyclic finite element analysis

The goal of the topology optimization was to develop new structural fuse shapes that resist buckling and promote yielding when subjected to cyclic deformation. To evaluate whether the optimized topologies shown in Fig. 5 satisfy that goal, it is necessary to perform 3D material-nonlinear and geometrically-nonlinear analysis. First, each optimized topology is converted into a smooth version of its coarse predecessor (as illustrated in Fig. 6) to eliminate stress localization at reentrant pixelated corners. Simple geometric entities such as lines, circles, ellipses and three-point arcs are used to interpret the topologies. Then, two solid boundary elements are added at the top and bottom of each topology to facilitate application of boundary conditions. Finite element models are created with the Abaqus software (Simulia 2014) using full integration four-node shell elements with an approximate size of 12 mm. The material is modeled as elastic isotropic with a nonlinear kinematic hardening rule representative of ASTM A572 Grade 50 steel plate material as described in Section 2. To account for geometric imperfections in the plate, the first buckling mode is scaled by a factor of $h/250$ and used as an initial imperfection in each model. Due to potential large deformations related to buckling, geometric nonlinearity is included. Lateral displacements are applied at the reference point located at the middle of the top boundary element and the displacement protocol is an adaptation of the qualifying cyclic test protocol for link-to-column moment connections in eccentrically braced frames (AISC 2016). The static general solver (implicit algorithm) is used to run the cyclic analysis.

For the optimized topologies with a value of $k=0.1$ and 0.2 , the plastic deformations are localized in both ends of the two horizontal links as well as in the vertical legs, as shown in Fig. 6(a) and Fig. 6(b), respectively, wherein colors green through red indicate yielding. On the other hand, the optimized topology associated with a value of $k=0.3$, exhibits distributed plastic deformations along the mid-height of the fuse, as shown in Fig. 6(c). For comparison purposes, Fig. 6(d) shows four plastic hinges formed in a ring-shape structural fuse, located at the top and bottom of the sides of the ring (Egorova et al. 2014). Similarly, Fig. 6(e) shows a butterfly-shape structural fuse with plastic deformations initiating at quarter points of the links (Ma et al. 2010).

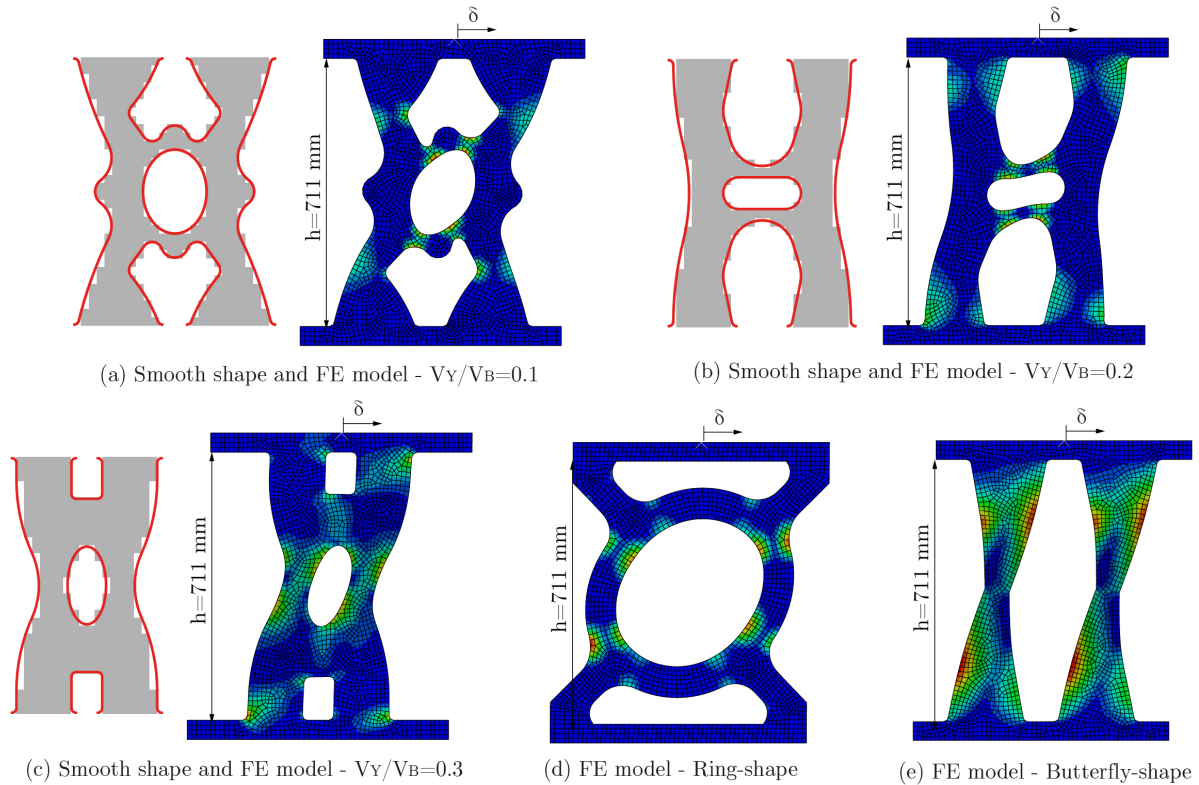


Figure 6: Smooth representation and FE models

The cyclic response of the optimized topologies is presented in Fig. 7(a) to Fig. 7(c). It is observed that the hysteretic shape varies from a full and stable hysteretic response for $k=0.1$ to a pinched behavior for $k=0.3$. Since the pinching behavior indicates out-of-plane buckling, this demonstrates the effectiveness of the topology optimization at controlling the amount of buckling resistance. For seismic structural fuses subjected to especially large shear angles, a topology like Fig. 6(a) might be ideal for resisting buckling and dissipating seismic energy. A structural fuse like shown in Fig. 6(b) exhibits full hysteretic behavior and buckling resistance up to shear angles of 4% to 5% (see Fig. 7(b)). This may be desirable for some applications, particularly because there is less growth in strength past yield which means smaller demands on surrounding elements. Conversely, values of $k \geq 0.3$ will produce hysteretic behavior that pinches at small shear angles and may not present many advantages compared to ring-shaped or butterfly-shaped structural fuses (comparing Fig. 7(c) and 7(d)). One advantage of all the optimized shapes, is that none of them exhibited significant stiffness degradation; in contrast, the

stiffness of the ring-shape fuse degraded and was 48% smaller at the end of the analysis as compared to the initial stiffness.

The effect of varying k from 0.1 to 0.3 is also noticeable in Fig. 7 as the yield strength increases by a factor of approximately 2.7. As discussed in the previous section, the shear buckling load remains fairly consistent between the three optimized topologies while the yielding mechanism and associated yield strength vary. Analyses (not shown here) have proven that the ratio of V_Y/V_B varies linearly with the scale of the structural fuse (Avecillas 2018). That is, if a stronger fuse is desired, all dimensions of the fuse can be scaled up and the buckling behavior (e.g. hysteretic shape) should remain relatively constant. Alternatively, additional strength could be obtained by repeating the topology in the same plane or in parallel plates.

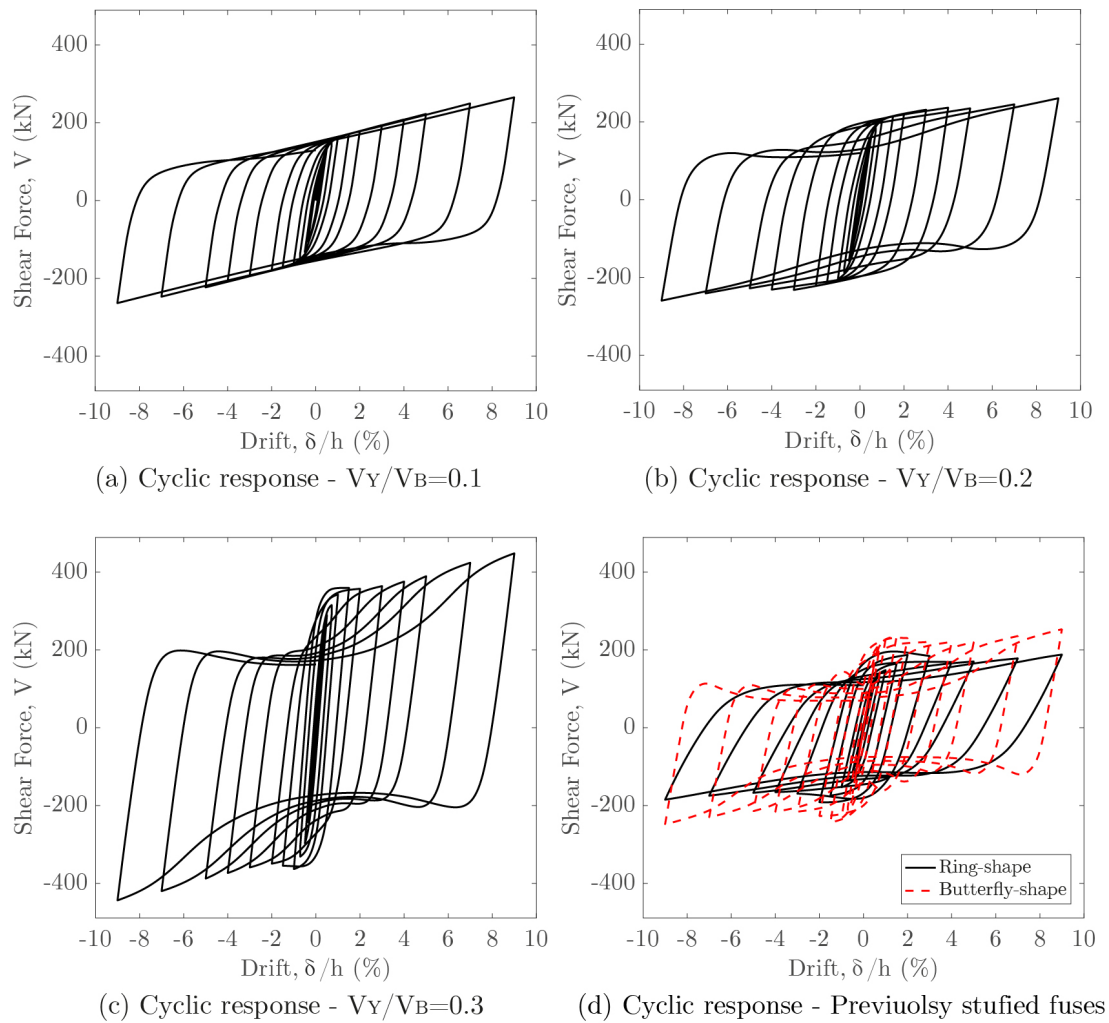


Figure 7: Cyclic response of the structural fuses

The backbone curves corresponding to the five structural fuses analyzed in this study are presented in Fig. 8(a). It is observed that the optimized topologies have a greater initial stiffness than the ring-shape structural fuse. Also, the optimized topologies have a greater initial stiffness with larger values of k . The cumulative dissipated energy per volume of material, Fig. 8(b) can

be used as a metric to evaluate the effectiveness of material in the new fuse shapes. From Fig. 8(b) it is observed that at the end of the loading protocol, the optimized topologies dissipate a minimum of 48 Nmm/mm^3 whereas the ring-shape and butterfly-shape structural fuses only dissipate 36 Nmm/mm^3 and 40 Nmm/mm^3 , respectively. Along the same lines, Fig. 8(c) shows that the optimized topologies corresponding to $k=0.1$ and $k=0.2$, produce more equivalent viscous damping than the ring-shaped or butterfly-shaped topologies. The optimized topology with $k=0.3$ and the butterfly-shaped topology show the largest decay in equivalent viscous damping due to buckling and pinched behavior for shear angles larger than 3%.

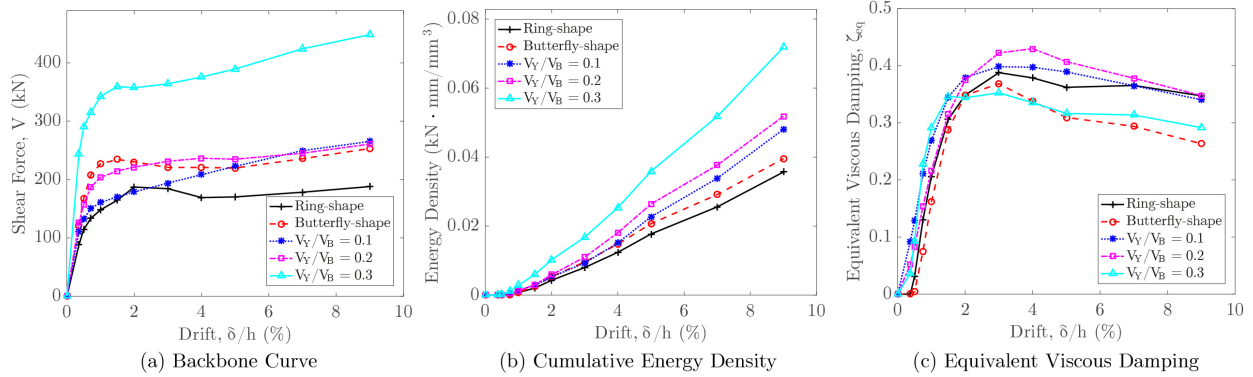


Figure 8: Backbone curve, dissipated energy and damping capacity

Finally, Fig. 9 shows the distribution of equivalent plastic strains at the end of the loading protocol. These values can be viewed as cumulative plastic strains and are presented to give a comparative assessment of fracture potential but not intended to predict when fracture would occur. In that context, it is shown that the topology with $k=0.3$ has its worst equivalent plastic strain at the base of the legs whereas the topologies with $k=0.2$ and $k=0.1$ reach their maximum equivalent plastic strains at the ends of the horizontal ties with values that are 2.4 and 3.3 times larger than the $k=0.3$ topology, respectively. The large equivalent plastic strains imply that the $k=0.1$ and $k=0.2$ topologies would likely experience some fracture before reaching the end of the loading protocol.

It is noted that the objective function did not include consideration for minimizing equivalent plastic strain, so it is not surprising that the plastic strains are large. Several approaches are possible for limiting the potential for fracture including: 1) incorporate the equivalent plastic strain into the objective function, 2) adjust the optimized topologies by tweaking dimensions, curves, or shapes to reduce plastic strains, or 3) reimagine the optimized topology in a form that retains its buckling resistance while incorporating concepts from previous structural fuse shapes that reduce plastic strains. This is the subject of ongoing research.

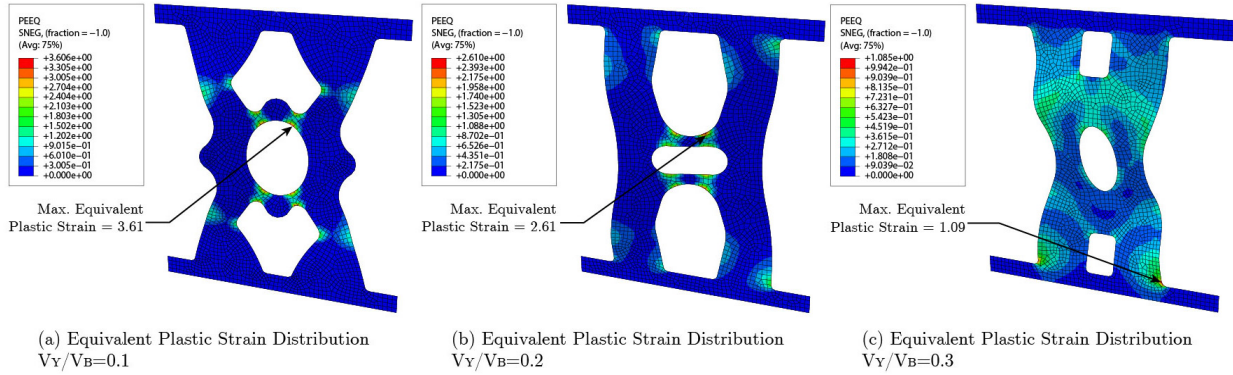


Figure 9: Distribution of equivalent plastic strains in the optimized topologies

5. Conclusions

Shear-acting structural fuses are thin steel plates subjected to in-plane lateral displacements that dissipate energy through localized shear or flexural yielding mechanisms. However, these structural components can be prone to undesirable buckling at small levels of drift angles.

This study uses topology optimization to create new shapes for structural fuses that resist buckling. An objective function was developed based on two values: 1) shear buckling load, V_B , obtained from an eigenvalue analysis, and 2) shear yield load, V_Y , obtained from a 2D material-nonlinear analysis. The ratio V_Y/V_B was found to control the amount of cyclic deformation that is possible before buckling occurs and the analyses were computationally efficient enough for implementation in an optimization routine. Using a genetic algorithm based topology optimization procedure, several topologies were produced with varying resistance to buckling (i.e. varying target values for V_Y/V_B from 0.1 to 0.3).

Based on a square domain and 40% volume ratio, the resulting optimized topologies showed that the best shape for resisting buckling consists of two vertical legs with two horizontal ties spanning between them. The optimized topology with target ratio of $V_Y/V_B=0.3$ did not have a clear plastic mechanism and experienced buckling and hysteretic pinching such that it is not clear that this topology has advantages compared to topologies found in the literature (e.g. butterfly-shaped or ring-shaped structural fuses). The optimized topologies with target ratio of $V_Y/V_B=0.2$ and 0.1, on the other hand, exhibited excellent buckling resistance up to 9% and 4% shear angle, respectively, and demonstrated stable full hysteretic shape, and increased energy dissipation. One challenge related to the optimized topologies is localized large equivalent plastic strains which suggest more work needs to be done to limit the potential for fracture.

Acknowledgments

Thanks to The National Secretariat of Higher Education, Science, Technology, and Innovation of Ecuador (SENESCYT) for the support provided through its graduate fellowship program. Some aspects of this work were supported by the National Science Foundation under Grant No. CMMI-1453960. Any opinions, findings, and conclusions or recommendations expressed in this material are those of the authors and do not necessarily reflect the views of the National Science Foundation or other sponsors.

References

- AISC (2016). "Seismic provision for structural steel buildings." *ANSI/AISC 341-16*.
- Avecillas, J. (2018). "Topology optimization of steel shear fuses to resist buckling". Master's thesis. *Virginia Polytechnic Institute and State University*.
- Deng, K., Pan, P., Li, W. and Xue, Y. (2015). "Development of a buckling restrained shear panel damper." *Journal of Constructional Steel Research*, 106(1), 311-321.
- Egorova, N., Eatherton, M. R. and Maurya, A. (2014). "Experimental study of ring-shaped steel plate shear walls." *Journal of Constructional Steel Research*, 103, 179-189.
- Ghabraie, K., Chan, R., Huang, X. and Xie, Y. M. (2010). "Shape optimization of metallic yielding devices for passive mitigation of seismic energy." *Engineering Structures*, 32(8), 2258-2267.
- Liu, Y. and Shimoda, M. (2013). "Shape optimization of shear panel damper for improving the deformation ability under cyclic loading." *Structural and Multidisciplinary Optimization*, 48(2), 427-435.
- Ma, X., Borchers, E., Pena, A., Krawinkler, H. and Deierlein, G. (2010). "Design and behavior of steel shear plates with openings as energy-dissipating fuses." *John A. Blume Earthquake Engineering Center Technical Report*, (173).
- Madeira, J. A., Rodrigues, H. and Pina, H. (2006). "Multi-objective topology optimization of structures using genetic algorithms with chromosome repairing." *Structural and Multidisciplinary Optimization*, 32(1), 31-39.
- Sigmund, O. (2001). "A 99 line topology optimization code written in Matlab." *Structural and multidisciplinary optimization*, 21(2), 120-127.
- Simulia (2014). "Abaqus version 6.14 documentation" *Dassault Systems*.
- Taylor, R. L. (2013). "Feap version 8.4 user manual." *University of California at Berkeley*.